



ORIGINAL RESEARCH ARTICLE

Osteoporosis and osteoblasts cocultured with adipocytes inhibit osteoblast differentiation by downregulating histone acetylation

Rodrigo P. F. Abuna | Luciana O. Almeida | Alann T. P. Souza | Roger R. Fernandes |
Thales F. V. Sverzut | Adalberto L. Rosa | Marcio M. Beloti

Bone Research Lab, School of Dentistry of
Ribeirão Preto, University of São Paulo,
Ribeirão Preto, São Paulo, Brazil

Correspondence

Marcio M. Beloti, Bone Research Lab, School of
Dentistry of Ribeirão Preto, University of São
Paulo, Av. do Café s/n, Ribeirão Preto,
SP 14040-904, Brazil.
Email: mmbeloti@usp.br

Funding information

Conselho Nacional de Desenvolvimento
Científico e Tecnológico,
Grant/Award Number: 303464/2016-0;
Coordenação de Aperfeiçoamento de Pessoal
de Nível Superior; Fundação de Amparo à
Pesquisa do Estado de São Paulo,
Grant/Award Numbers: 2016/14171-0, 2016/
14711-4, 2017/12622-7, 2018/13290-0,
2018/17356-6

Abstract

Osteoporosis is characterized by decreased bone mass and adipocyte accumulation within the bone marrow that inhibits osteoblast maturation, leading to a high risk of fractures. Thus, we hypothesized that osteoblasts, besides being negatively affected by interacting with adipocytes, reduce the differentiation of neighboring osteoblasts through the same mechanisms that affect osteoblasts under osteoporotic conditions. We investigated the effect of osteoporosis on osteoblast differentiation and the effect of the conditioned medium of osteoblasts cocultured with adipocytes on the differentiation of other osteoblasts. Osteoporosis was induced by orchietomy in rats and bone marrow mesenchymal stromal cells (MSCs) were differentiated into osteoblasts. Also, the bone marrow and adipose tissue MSCs were obtained from healthy rats and differentiated into osteoblasts and adipocytes, respectively. Messenger RNA expression, in situ alkaline phosphatase activity, and mineralization confirmed the inhibitory effect of osteoporosis on osteoblast differentiation. This harmful effect was mimicked by the in vitro model using the conditioned medium and it was demonstrated that osteoblasts keep the memory of the negative impact of interacting with adipocytes, revealing an unknown mechanism relevant to the osteoporotic bone loss. Finally, we showed the involvement of acetyl-histone 3 (AcH3) in bone homeostasis as its reduction induced by osteoporosis and conditioned medium impaired osteoblast differentiation. The AcH3 involvement was proved by treating osteoblasts with Trichostatin A that recovered the AcH3 expression and osteoblast differentiation capacity in both situations. Together, our findings indicated that AcH3 might be a target for future studies focused on epigenetic-based therapies to treat bone diseases.

KEYWORDS

adipocyte, histone, mesenchymal stromal cell, osteoblast, osteoporosis

1 | INTRODUCTION

Osteoporosis is a metabolic bone disorder characterized by the disruption in the balance between bone formation and resorption,

leading to a decreased bone mass and a high risk of fractures. Although it is more common in women and the elderly, it also affects men and people of all age groups (Hahn, 1988; Vondracek & Linnebur, 2009). A peculiarity observed in both aging and the

osteoporotic condition is the accumulation of medullary adipocytes with increasing bone loss (Al Saedi et al., 2020; Justesen et al., 2001; Meunier et al., 1971). This phenomenon is attributed to the fate decision of mesenchymal stromal cells (MSCs) in favor of adipocytes at the expense of osteoblasts (Bennett et al., 1991). Fortunately, there are also regulators in these lineages to balance the cell fate switching, promoting osteoblastogenesis while suppressing adipogenesis (Muruganandan et al., 2009; Takada et al., 2007).

Within the bone tissue microenvironment, osteoblasts, osteoclasts, and osteocytes secrete signaling molecules that act as autocrine, paracrine, and endocrine signals for the maintenance of skeletal homeostasis and architecture (Han et al., 2018). Remarkably, adipocytes either cohabiting with this heterogeneous population or from distant sites secrete factors, such as adiponectin, leptin, and proinflammatory cytokines, including tumor necrosis factor- α (TNF- α) and interleukin-6 (IL6) that negatively impact osteoblast differentiation (Abuna et al., 2016; Rosen & Bouxsein, 2006). Several of these factors can disrupt bone homeostasis in which some cytokines are associated with osteoporosis (Kotrych et al., 2016; Manolagas et al., 1995; Tyagi et al., 2012). Additionally, the microenvironment acts on the epigenetic regulation of the cells, affecting the expression of genes that drive bone biology and diseases (Montecino et al., 2015). The deletion of histone deacetylase (HDAC) 3 in mice prevents limb lengthening and affects signaling pathways involved in endochondral and intramembranous bone formation (Feigenson et al., 2017). The inhibition of HDACs in human periodontal ligament cells enhances bone repair when implanted in mouse calvarial bone defects (Huynh, Everts, Nifuji, et al., 2017). In culture cell models, components in the serum can regulate histone modifications and the dynamics of the chromatin that controls gene expression (Zippo et al., 2009). MSCs cultured in autologous serum increased osteogenic differentiation; whereas, MSCs cultured in fetal bovine serum have increased adipogenic potential, both regulated by different profiles of histone modifications at the promoter of gene targets that were influenced by different serum conditions (Fani et al., 2016).

In osteoporosis and aging, adipocytes accumulate within the bone marrow and affect bone remodeling, partly by inhibiting osteoblast activity (Al Saedi et al., 2020). We hypothesized that as a consequence of their interactions with adipocytes, osteoblasts impair the differentiation of neighboring osteoblasts, and this contributes to osteoporotic bone loss. Additionally, the underlying cellular mechanisms were hypothesized to be the same as those that affect osteoblasts under osteoporotic conditions. To test these hypotheses, firstly, we evaluated the osteogenic potential of MSCs derived from osteoporotic rats that continued to switch their differentiation in favor of adipogenesis even when cultured in an osteogenic medium. Then, we created an *in vitro* model to determine the effects of a conditioned medium of osteoblasts cocultured with adipocytes on osteoblasts grown in nonconditioned medium. Our results demonstrated that osteoblasts indeed retained the impact of interacting with adipocytes, which inhibited the differentiation of other osteoblasts in the same way as osteoporosis, that is, by reducing histone acetylation.

2 | MATERIALS AND METHODS

2.1 | Animals and experimental design

All procedures involving animals were approved by the Committee of Ethics in Animal Research of the School of Dentistry of Ribeirão Preto, University of São Paulo (Protocol #2018.1.30.58.8) and followed all national/international guidelines for animal care. In this study, 24 male 4-week-old Wistar rats with approximately 150 g of body weight were used. During the entire period, the animals were kept under constant temperature ($22 \pm 2^\circ\text{C}$) and received food and water *ad libitum*. The whole experimental design is presented in Figure S1.

2.2 | Effect of osteoporosis on bone morphometric parameters

2.2.1 | Surgical procedure to induce osteoporosis

Osteoporosis was induced in eight rats through bilateral orchietomy surgery (ORX). The animals were anesthetized with intraperitoneal injections of coopazine anesthetic solution (xylazine; Agibrands do Brasil Ltda.) and the analgesic muscle relaxant dopalen (ketamine; Agibrands) at dosages of 0.6 mg/100 g and 7.5 mg/100 g of body weight, respectively. Preoperative analgesia was performed with flunixinmeglumine, 0.25 mg/100 g of body weight (banamine; Schering-Plough) to proceed with the standard orchietomy technique (Zarrow et al., 1964). The anterior region of the scrotum was incised, and the vaginal tunic opened to exteriorize the testicles. Subsequently, the spermatic funicles were connected with 3-0 silk thread (Ethicon Ltda.) and sectioned at the height of the vas deferens. The testicles and epididymis were removed, and the skin of the scrotum was sutured. Eight animals, designated as Sham, underwent a fictitious orchietomy surgery; wherein, an incision was made in the scrotum to expose the testicles followed by the closure. Thereafter, the animals were medicated with a single dose of flunixinmeglumine 100 mg/100 g of body weight (Schering) and an antibiotic solution containing benzyl benzylpenicillin (156,000 IU/100 g of body weight), benzylpenicillin procaine (78,000 IU/100 g of body weight), benzylpenicillin potassium (78,000 IU/100 g of body weight), dihydrostreptomycin base sulfate (65 mg/100 g of body weight), and streptomycin base sulfate (65 mg/100 g of body weight) (pentabiotic; Fort Dodge). The animals were kept in the animal facilities for 90 days postoperatively, a period necessary for developing osteoporosis.

2.2.2 | Bone morphometry by microcomputed tomography (μCT) analysis

Osteoporosis was confirmed by microtomographic and morphometric analyses of the femurs from ORX and Sham rats. The region selected for measurements started at the metaphysis, 0.5 mm from

the end of the growth plate, and continued for 2 mm toward the diaphysis. The measurements were done in the trabecular region as the initial bone loss associated with sex-steroid deficiency is reportedly observed in that region predominantly, and only with aging is the cortical bone affected (Riggs et al., 2008). After euthanasia ($n = 6$ per group), the femurs were removed and stored in 10% formalin buffered with 0.1 M sodium cacodylate, pH 7.0 (Merck, HE). The high-resolution SkyScan 1172 microtomograph (Bruker) and the NRecon software (version 1.6.10.4; Bruker) were used to scan the samples and reconstruct the images, respectively. The parameters of the μ CT scan acquisition were: voxel size, $9.92 \mu\text{m}^3$; source voltage, 59 kVp; source current, 165 mA; filter, Al 0.5 mm; exposure, 610 ms; rotation step, 0.3° ; frame averaging, $4n$; and random movement, 10. Thereafter, the morphometric parameters, namely, bone volume (BV), bone volume/total volume (BV/TV), bone surface (BS), bone mineral density (BMD), trabecular number (Tb.N), trabecular thickness (Tb.Th), and trabecular separation (Tb.Sp), were analyzed by the CTAn software (version 1.15.4.0; Bruker). The μ CT analysis was done following previously described guidelines (Bouxsein et al., 2010; Dempster et al., 2013).

2.3 | Effect of osteoporosis on osteoblasts

2.3.1 | Harvesting, culture, and osteoblast differentiation of bone marrow MSCs

To obtain bone marrow MSCs, after euthanasia of Sham and ORX rats ($n = 4$ per group), 90 days postoperatively, the femurs were removed, both epiphyses were cut, and the medullary canals were flushed. The cells were cultured in a growth medium, composed of alpha minimum essential medium (α -MEM; Gibco), 10% fetal calf serum (Gibco), 1% penicillin-streptomycin (Gibco), and 0.3 mg/ml fungizone (Gibco) until 80% confluence. Then, the cells were enzymatically detached and osteoblast differentiation was induced for up to 17 days by plating them in six-well culture plates (Corning Incorporated) at a cell density of 1×10^5 cells/well in an osteogenic medium, comprising growth medium, 50 $\mu\text{g}/\text{ml}$ ascorbic acid (Gibco), 7 mM β -glycerophosphate (Sigma-Aldrich), and 10^{-7} M dexamethasone (Sigma-Aldrich). The medium was replaced every 2 days and cells were kept in an incubator at 37°C , 95% O_2 , and 5% CO_2 .

2.3.2 | Messenger RNA (mRNA) expression by real-time polymerase chain reaction (RT-qPCR)

Transcripts corresponding to key osteoblast and adipocyte markers, as well as cytokines and histone components (Table 1), were analyzed by RT-qPCR on Day 10. Total RNA was extracted with Trizol reagent (Invitrogen) and the complementary DNA (cDNA) was generated from 1 μg extracted RNA using the High-Capacity cDNA Reverse Transcription Kit (Applied Biosystems). Then, RT-qPCR ($n = 3$) was carried out in Step One Plus Real-Time PCR system (Thermo Fisher

TABLE 1 TaqMan probes for real-time polymerase chain reaction

Gene	Gene name	Identification
<i>Runx2</i>	Runt-related transcription factor 2 (<i>Runx2</i>)	Rn01512298_m1
<i>Sp7</i>	Sp7 transcription factor (Osterix, <i>Sp7</i>)	Rn02769744_s1
<i>Alpl</i>	Alkaline phosphatase (<i>Alp</i>)	Rn01516028_m1
<i>Ibsp</i>	Integrin-binding sialoprotein (Bone sialoprotein, <i>Bsp</i>)	Rn00561414_m1
<i>Spp1</i>	Secreted phosphoprotein 1 (Osteopontin, <i>Opn</i>)	Rn00681031_m1
<i>Pparg</i>	Peroxisome proliferator-activated receptor gamma (<i>Pparγ</i>)	Rn00440945_m1
<i>Fabp4</i>	Fatty acid-binding protein 4 (Adipocyte protein 2, <i>Ap2</i>)	Rn00670361_m1
<i>Retn</i>	Resistin (<i>Retn</i>)	Rn00595224_m1
<i>Adipoq</i>	Adiponectin, C1Q, and collagen domain-containing (<i>Adipoq</i>)	Rn00595250_m1
<i>Tgfb1</i>	Transforming growth factor-beta 1 (<i>Tgfb1</i>)	Rn00572010_m1
<i>Il10</i>	Interleukin 10 (<i>Il10</i>)	Rn01483988_g1
<i>Il1B</i>	Interleukin 1 beta (<i>Il1β</i>)	Rn00580432_m1
<i>Il6</i>	Interleukin 6 (<i>Il6</i>)	Rn01410330_m1
<i>Tnf</i>	Tumor necrosis factor (<i>TNF-α</i>)	Rn01525859_g1
<i>Nfkb1</i>	Nuclear factor of kappa light polypeptide gene enhancer in B-cells 1 (<i>NF-κb</i>)	Rn01399572_m1
<i>Sirt1</i>	Sirtuin 1 (<i>Sirt1</i>)	Rn01428096_m1
<i>Hdac1</i>	Histone deacetylase 1 (<i>Hdac1</i>)	Rn01519308_g1
<i>Hdac2</i>	Histone deacetylase 2 (<i>Hdac2</i>)	Rn01193634_g1
<i>Actb</i>	Actin beta (β -actin)	Rn00667869_m1

Scientific) using TaqMan PCR Master Mix (Applied Biosystems) and probes for the target genes. All transcripts were normalized to *Actb* and the data were expressed as relative mRNA expression by using the cycle threshold method ($2^{-\Delta\Delta C_t}$).

2.3.3 | In situ alkaline phosphatase (ALP) activity by fast red staining

In situ ALP activity was evaluated on Day 10 by fast red staining. Briefly, a solution of Fast Red-TR reagent (Sigma-Aldrich) and Naphthol AS-MX phosphate (Sigma-Aldrich) was added to the samples for 30 min, following which they were washed and dried at room temperature. Images of the samples were acquired in an epifluorescence light microscope Axio Imager M2 Zeiss (Carl Zeiss, Inc.). The average of five random stained areas of three wells ($n = 5$) was used to quantify the pixels by using the ImageJ 1.52 software (National Institute of Mental Health) and the data were expressed as a percentage of area.

2.3.4 | Extracellular matrix mineralization by alizarin red S staining

The extracellular matrix mineralization was evaluated on Day 17 using alizarin red S staining (Sigma-Aldrich). The cells were fixed with 70% alcohol for 1 h, at 4°C, followed by the addition of alizarin red S solution for 15 min. Thereafter, the samples were washed and dried at room temperature and images of the samples were acquired as described for ALP activity. The calcium content was detected using a colorimetric assay (Gregory et al., 2004). Briefly, the staining was extracted by 10% acetic acid; the resulting solution was vortexed, heated at 85°C, cooled at 4°C, and centrifuged at 13,000g for 15 min. The supernatant was mixed with 10% ammonium hydroxide and this solution was read at 405 nm in a plate reader μ Quant (Bio-Tek Instruments Inc.). The data ($n = 5$) were expressed as absorbance.

2.3.5 | HDAC1 protein expression by western blot analysis

The Western blot analysis was carried out on Day 12, following the conventional protocol. Primary mouse monoclonal antibody anti-HDAC1 (5356S, 10E2, 1:1000; Cell Signaling) was used to detect HDAC1 protein, followed by the secondary anti-mouse immunoglobulin G-horseradish peroxidase (IgG HRP)-linked antibody (7076S, 1:2000; Cell Signaling). As a control, glyceraldehyde 3-phosphate dehydrogenase (GAPDH) protein was detected with a primary rabbit polyclonal anti-GAPDH antibody (sc25778, FL335, 1:2000; Santa Cruz Biotechnology). The images were acquired using G-Box gel imaging (Syngene) and the proteins were quantified ($n = 3$) by counting pixels and normalized by GAPDH.

2.3.6 | Acetyl-histone 3 (ACh3) and nuclear factor- κ B (NF- κ B) protein expression by immunofluorescence labeling

The ACh3 protein was detected on Day 12 by indirect immunofluorescence with the primary rabbit monoclonal antibody anti-ACh3 (Lys9, C5B11, 1:400; Cell Signaling), followed by Alexa Fluor 594-conjugated secondary anti-rabbit IgG HRP antibody (7074S, 1:800; Cell Signaling). The nuclei were stained with blue fluorescent 4',6-diamidino-2-phenylindole dihydrochloride (DAPI; D3571, 1:300; Molecular Probes). Three samples were observed, and random images were acquired as described above.

The NF- κ B protein expression is presented as a supplemental file and it was detected on Day 12 with primary rabbit monoclonal antibody NF- κ B (D14E12, 1:50; Cell Signaling), followed by Alexa Fluor 594-conjugated secondary anti-rabbit IgG HRP antibody (7074S, 1:800; Cell Signaling). The actin cytoskeleton was stained with Alexa Fluor 488-conjugated phalloidin (A12379, 1:200; Molecular Probes) and the nuclei with DAPI as described above.

2.4 | Effect of conditioned medium of osteoblasts cocultured with adipocytes on osteoblasts

2.4.1 | Harvesting, culture, and adipocyte differentiation of adipose tissue MSCs

After euthanasia of four healthy 4-week-old Wistar rats, the inguinal adipose tissue was harvested to obtain MSCs. Briefly, the enzymatic digestion of the tissue was done by using 0.075% collagenase type II (Gibco), at 37°C for 40 min. The fat was centrifuged, the supernatant containing floating adipocytes were discarded, and the pellet was re-suspended in growth medium and cultured until 80% confluence. Thereafter, the cells were enzymatically detached and adipocyte differentiation was induced for up to 7 days by plating them in six transwell porous filters (Corning Incorporated) at a cell density of 2×10^5 cells/well in an adipogenic medium comprising Dulbecco's modified Eagle medium (DMEM; Gibco), 10% fetal calf serum (Gibco), 1% penicillin-streptomycin (Gibco), 0.3 mg/ml fungizone (Gibco), 10^{-6} M dexamethasone (Sigma-Aldrich), 0.5 μ M 3-isobutyl-1-methylxanthine (Sigma-Aldrich), 10 mg/ml of insulin (Sigma-Aldrich), and 0.1 M indomethacin (Sigma-Aldrich). This medium was reported to be suitable for inducing adipocyte differentiation of adipose tissue MSCs (Abuna et al., 2016; Freitas et al., 2020). It was replaced every 2 days and the cells were kept in an incubator at 37°C, 95% O₂, and 5% CO₂.

2.4.2 | Coculture and generation of the conditioned medium

After obtaining osteoblasts and adipocytes as described above, they were indirectly cocultured. This was done by placing the adipocytes that were in the transwell porous filters into the six-well culture plates (Corning Incorporated) containing osteoblasts and keeping them in the osteogenic medium for 3 days. Thereafter, the transwell porous filters containing adipocytes were removed and to generate the conditioned medium, the previously cocultured osteoblasts were cultured in serum-free α -MEM (Gibco) supplemented with 1% penicillin-streptomycin (Gibco) and 0.3 mg/ml fungizone (Gibco) for 24 h. This conditioned medium was supplemented to an osteogenic medium and was used (100% conditioned medium) to culture another pool of osteoblasts that had already been cultured for 7 days, for an additional 3 days. Hence, the total culture period was 10 days. The osteoblasts were not treated with CM before Day 7 to prevent interference with the initial events of osteoblast differentiation of bone marrow MSCs. The use of a conditioned medium during this specific stage of the cell culture was based on a previous study where we demonstrated that 3 days of coculture was suitable to elicit the negative effect of adipocytes on osteoblast differentiation (Abuna et al., 2016). The osteogenic conditioned medium was then replaced by an osteogenic medium and the osteoblasts were cultured up to day 17. Osteoblasts grown in an osteogenic medium during the entire period were used as control.

The medium was replaced every 2 days or when indicated, and the cells were kept in an incubator at 37°C, 95% O₂, and 5% CO₂. The same assays used to evaluate the effect of osteoporosis on osteoblasts were also performed to evaluate the effect of conditioned medium of osteoblasts cocultured with adipocytes on osteoblasts.

2.5 | Participation of histone acetylation on decreased osteoblast differentiation induced by osteoporosis and conditioned medium of osteoblasts cocultured with adipocytes

To investigate if Ach3 reduction is involved in the decreased osteoblast differentiation induced by osteoporosis in vivo or the conditioned medium in vitro, bone marrow MSCs from Sham and ORX rats were cultured for 10 days in osteogenic medium, as described above, and treated with 100 nM trichostatin A (TSA; Sigma-Aldrich), an inhibitor of HDAC, in the last 24 h. Also, bone marrow MSCs from healthy rats were cultured in osteogenic medium for 7 days, followed by 3 days in conditioned medium and an additional day in osteogenic medium supplemented with 100 nM TSA (Sigma-Aldrich). Thereafter, the protein expression of Ach3 and runt-related transcription factor 2 (RUNX2) were evaluated by Western blot analysis and the in situ ALP activity was detected as described above.

2.5.1 | Ach3 and RUNX2 protein expression by Western blot analysis

The Western blot analysis was carried out on Day 11, following the conventional protocol. Primary rabbit monoclonal antibodies anti-RUNX2 (8486 S, D1H7, 1:2000; Cell Signaling) and anti-Ach3 (Lys9, 9649, 1:1000; Cell Signaling) were used to detect RUNX2 and Ach3 proteins, respectively. For both, a secondary antirabbit IgG HRP antibody (1:4000; Cell Signaling) was used. As a control for RUNX2, GAPDH protein was detected with a primary rabbit polyclonal anti-GAPDH antibody (sc25778, FL335, 1:2000; Santa Cruz Biotechnology). As a control for Ach3, anti-Histone 3 (H3) protein was detected with a primary rabbit monoclonal anti-H3 (4499S, D1H2, 1:4000; Cell Signaling). The images were acquired using G-Box gel imaging (Syngene) and the proteins were quantified (n = 3) by counting pixels and normalized by GAPDH or H3.

2.6 | Statistical analysis

The data were analyzed by either the Student's t test or one-way analysis of variance, followed by Student Newman Keuls posttest. The significance level was established at p ≤ .05. All experiments were performed a minimum of three times to ensure the validity of the data.

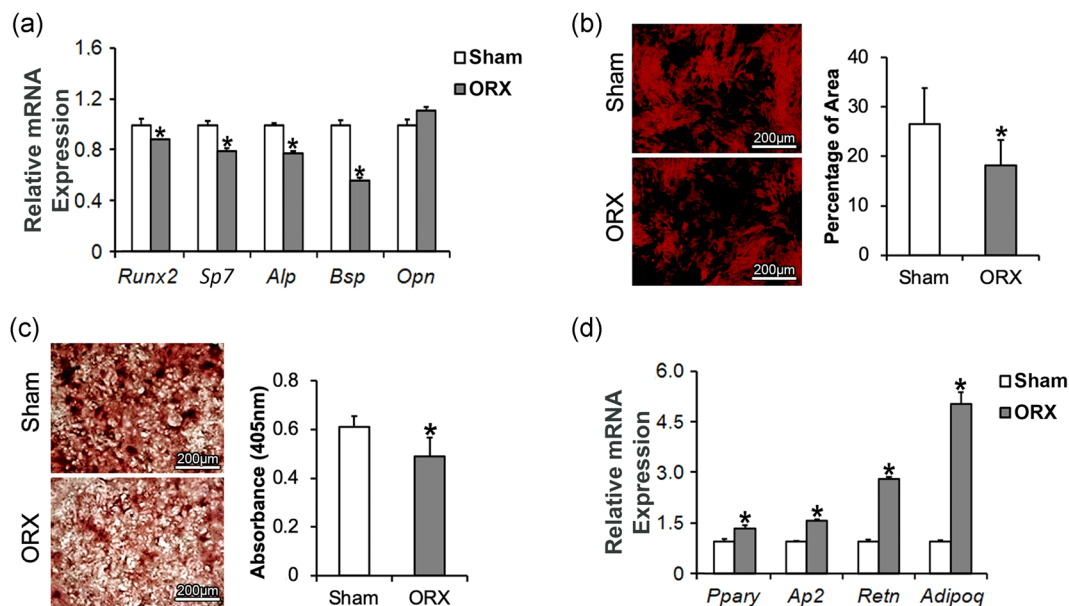


FIGURE 1 Effect of orchietomy on the osteogenic and adipogenic potential of osteoblasts differentiated from mesenchymal stromal cells. Messenger RNA (mRNA) expression of the bone markers *Runx2*, *Sp7*, *Alp*, *Bsp*, and *Opn* (a), in situ alkaline phosphatase (ALP) activity on Day 10 (b), and extracellular matrix mineralization on Day 17 (c) of osteoblasts derived from Sham and orchietomy surgery (ORX) rats. mRNA expression of the adipocyte markers *Ppary*, *Ap2*, *Retn*, and *Adipoq* of osteoblasts derived from Sham osteoporotic (ORX) rats on Day 10 (c). The data of mRNA (n = 3), in situ ALP activity (average of five random stained areas of three wells, n = 3), and extracellular matrix mineralization (n = 5) are presented as mean ± standard deviation. *Statistically significant differences between osteoblasts derived from Sham and ORX rats (p ≤ .05)

3 | RESULTS

3.1 | Effect of osteoporosis on osteoblasts

Ninety days postoperatively, the osteoporotic condition was confirmed by μ CT analysis and bone morphometric parameters (Figure S2). To investigate if osteoporosis affected the osteogenic potential of MSCs differentiating into osteoblasts, we evaluated the mRNA expression of key bone markers and found it to be downregulated for *Runx2* ($p = .0009$), osterix (*Sp7*; $p = .0094$), *Alp* ($p = .0173$), and bone sialoprotein (*Bsp*; $p = .0029$), whereas that of osteopontin (*Opn*; $p = .0614$) was not affected on Day 10 (Figure 1a). Additionally, osteoporosis reduced the in situ ALP activity ($p = .0002$) on Day 10 (Figure 1b) and the extracellular matrix mineralization ($p = .0180$) on Day 17 (Figure 1c). Confirming the inverse relationship between bone and fat formation, the mRNA expression of the adipocytic markers, peroxisome proliferator-activated receptor gamma (*Ppar γ* ; $p = .0201$), adipocyte protein 2 (*Ap2*; $p = .0013$), resistin (*Retn*; $p = .0010$), and adiponectin (*Adipoq*; $p = .0032$), was upregulated by osteoporosis on Day 10, even under osteogenic condition (Figure 1d).

It is known that osteoporosis may affect the synthesis of cytokines and growth factors by osteoblasts and that the epigenetic state

interferes with the cell fate (Noda et al., 1987). Herein, we evaluated and demonstrated that *IL6* ($p = .0034$), *TNF- α* ($p = .0034$), *Nf- κ B* ($p = .0002$), sirtuin 1 (*Sirt1*; $p = .0364$), histone deacetylase 1 (*Hdac1*; $p = .0013$), and histone deacetylase 2 (*Hdac2*; $p = .0006$) were upregulated, whereas transforming growth factor-beta 1 (*Tgf β 1*; $p = .3375$) interleukin 10 (*Il10*; $p = .8995$), and interleukin 1 beta (*Il1 β* ; $p = .3248$) were not affected by osteoporosis on Day 10 (Figure 2a). Additionally, the expression of HDAC1 protein was increased ($p = .0003$) by osteoporosis on Day 12 (Figure 2b). As we found an upregulation of the transcripts *Hdac1* and *Hdac2* and the HDAC1 protein level, we evaluated the ACh3 protein expression on Day 12 that was reduced by osteoporosis (Figure 2c).

3.2 | Effect of conditioned medium of osteoblasts cocultured with adipocytes on osteoblasts

Adipocytes from bone marrow may have self-promotive capabilities, inducing MSCs to differentiate into adipocytes at the expense of osteoblasts and metabolically suppressing osteoblastogenesis through the synthesis of cytokines, such as *TNF- α*

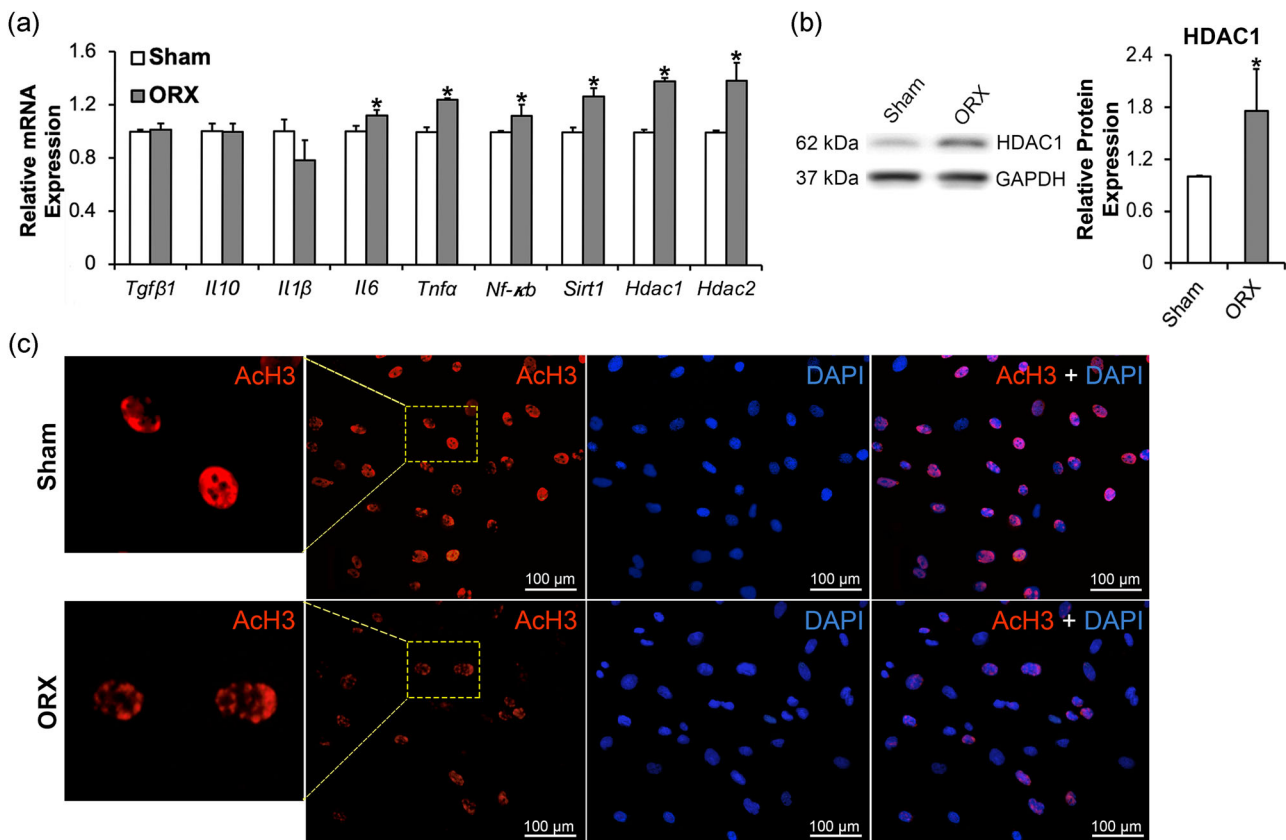


FIGURE 2 Effect of orchietomy on the expression of cytokines, histone deacetylases, and ACh3 by osteoblasts differentiated from MSCs. mRNA expression of the cytokines *Tgf β 1*, *Il10*, *Il1 β* , *Il-6*, *NF- κ B*, *TNF- α* , and *Sirt1* and histones deacetylases *Hdac1* and *Hdac2* on Day 10 (a), HDAC protein expression on Day 12 (b), and ACh3 protein expression on Day 12 (c) of osteoblasts derived from Sham and orchietomy surgery (ORX) rats. The data of mRNA ($n = 3$) is presented as mean \pm standard deviation. ACh3, acetyl-histone 3; GAPDH, glyceraldehyde 3-phosphate dehydrogenase; HDAC1, histone deacetylase; MSC, mesenchymal stromal cell; mRNA, messenger RNA. *Statistically significant difference between osteoblasts derived from Sham and ORX rats ($p \leq .05$)

(Abuna et al., 2016; Rosen et al., 2009). We designed an in vitro model attempting to mimic the effect of osteoporosis on osteoblasts by using a conditioned medium of osteoblasts cocultured with adipocytes in osteoblasts grown in nonconditioned medium. The mRNA expression of *Sp7* ($p = .0025$), *Alp* ($p = .0146$), and *Bsp* ($p = .0141$) was downregulated, whereas that of *Runx2* ($p = .6538$) and *Opn* ($p = .0626$) was not affected by the conditioned medium on Day 10 (Figure 3a). Additionally, the conditioned medium reduced the in situ ALP activity ($p = .0003$) on Day 10 (Figure 3b) and the extracellular matrix mineralization ($p = .0018$) on Day 17 (Figure 3c). As observed under osteoporotic condition, in osteoblasts cultured in conditioned medium, the mRNA expression of *Ppar γ* ($p = .0259$), *Ap2* ($p = .0460$), *Retn* ($p = .0049$), and *Adipoq* ($p = .0004$) was upregulated (Figure 3d).

As osteoporosis impacted osteoblasts in terms of cytokines and histone acetylation, we investigated if the conditioned medium could reproduce this effect on osteoblasts. The mRNA expression of *Il1 β* ($p = .0086$), *Il6* ($p = .0038$), *TNF- α* ($p = .0034$), *Nf- κ B* ($p = .0002$), *Sirt1* ($p = .0354$), *Hdac1* ($p = .0013$), and *Hdac2* ($p = .0006$) was upregulated, whereas that of *Tgfb β 1* ($p = .0788$) and *Il10* ($p = .1834$) was not affected by the conditioned medium on Day 10 (Figure 4a). The expression of HDAC1 protein was increased ($p = .0005$) (Figure 4b), whereas that of ACh3 protein was reduced on Day 12 (Figure 4c). Together, these results indicated that the proposed in vitro model recapitulated the effect of osteoporosis on osteoblasts in which the role of histone acetylation may be relevant in explaining the bone phenotype.

3.3 | Role of histone acetylation on decreased osteoblast differentiation induced by osteoporosis and conditioned medium of osteoblasts cocultured with adipocytes

As we observed reduced ACh3 expression concurrently with the decreased osteoblast differentiation induced by both osteoporosis and the conditioned medium, it is plausible that these two events shared the same mechanism. Histone deacetylation, catalyzed by HDAC, is associated with chromatin condensation and repression of transcriptional activity (Huynh, Everts, & Ampornaramveth, 2017). We hypothesized that ACh3 restoration by inhibiting HDACs reverts the disruption of osteoblast differentiation induced by osteoporosis and the conditioned medium, confirming the involvement of ACh3 in this process. We treated the osteoblasts with 100 nM TSA and analyzed the protein expression of ACh3 and RUNX2 as well as in situ ALP activity. The osteoporosis downregulated ($p = .0011$) the ACh3 protein expression that was recovered and increased ($p = .0001$) by TSA treatment (Figure 5a). The RUNX2 protein expression was not affected by osteoporosis ($p = 2.0352$) and it was upregulated ($p = .0004$) by TSA treatment under osteoporotic condition (Figure 5c). The in situ ALP activity was reduced ($p = .0009$) by osteoporosis that was increased ($p = .0004$) by TSA treatment but not fully restored (Figure 5e).

The effect of TSA treatment on osteoblasts cultured in the conditioned medium was similar to that on osteoblasts from

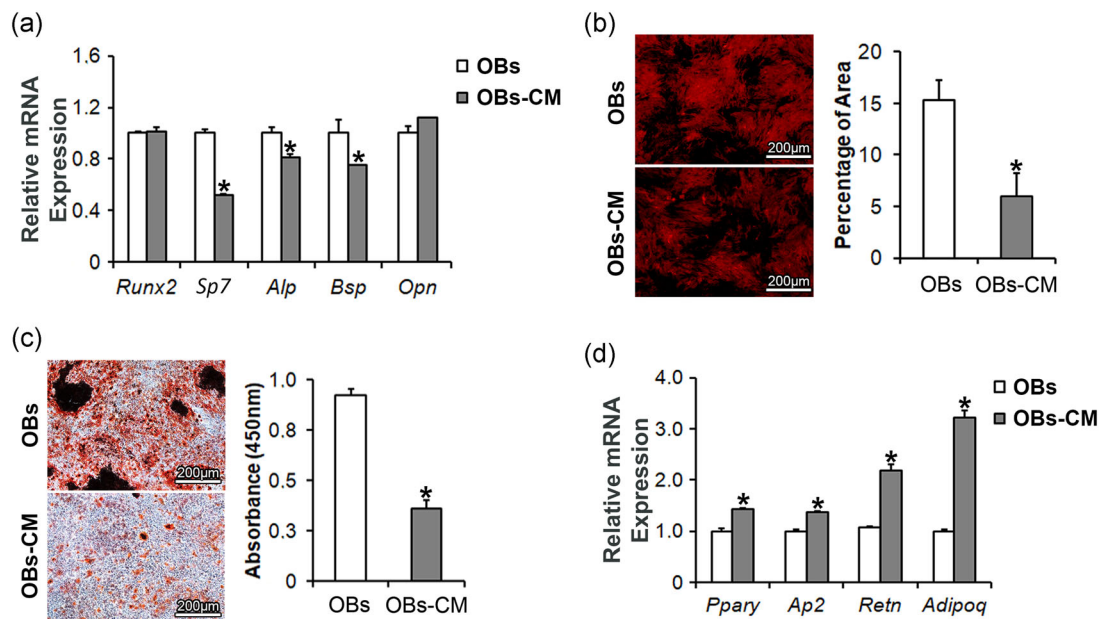


FIGURE 3 Effect of adipocytes (conditioned medium) on the osteogenic and adipogenic potential of osteoblasts differentiated from mesenchymal stromal cells. Messenger RNA (mRNA) expression of the bone markers *Runx2*, *Sp7*, *Alp*, *Bsp*, and *Opn* (a), in situ alkaline phosphatase (ALP) activity on Day 10 (b), and extracellular matrix mineralization on Day 17 (c) of osteoblasts cultured in nonconditioned medium (OBs) and osteoblasts cultured in conditioned medium (OBs-CM). mRNA expression of the adipocyte markers *Ppar γ* , *Ap2*, *Retn*, and *Adipoq* of OBs and OBs-CM on Day 10 (d). The data of mRNA ($n = 3$), in situ ALP activity (average of five random stained areas of three wells, $n = 3$), and extracellular matrix mineralization ($n = 5$) are presented as mean \pm standard deviation. *Statistically significant differences between OBs and OBs-CM ($p \leq .05$)

osteoporotic rats. The conditioned medium reduced the ACh3 ($p = .0029$) and RUNX2 ($p = .0001$) protein expressions that were recovered and increased ($p = .0001$ for ACh3 and $p = .0001$ for RUNX2) by TSA treatment (Figure 5b,d). The in situ ALP activity was reduced ($p = .0009$) by the conditioned medium that was increased ($p = .0001$) by TSA treatment, but not totally restored (Figure 5f). Together, these results confirmed our hypothesis and indicated the crucial involvement of loss of histone acetylation, mediated by the accumulation of HDAC, in the downregulation of osteoblast differentiation induced by osteoporosis that is mimicked by the conditioned medium generated by osteoblasts previously cocultured with adipocytes.

4 | DISCUSSION

Disruption of bone homeostasis can lead to bone loss and fat gain within the bone marrow microenvironment, ultimately contributing to a high risk of fractures as observed in osteoporosis (Al Saedi et al., 2020; Hahn, 1988; Muruganandan et al., 2009). We confirmed that osteoporosis reduced osteoblast differentiation of MSCs concomitantly with

increased adipogenic potential. Further, we established an in vitro model to determine the effects of a conditioned medium of osteoblasts cocultured with adipocytes on osteoblasts grown under osteogenic conditions. Interestingly, our findings indicated that osteoblasts seemed to retain their memory of their negative interaction with adipocytes that inhibits the differentiation of other osteoblasts, at least partly, through the same cellular mechanisms as osteoporosis, that is, by reducing ACh3 (Figure 6).

Steroid hormone deficiency produces osteoporosis type I, whereas age-related bone loss causes osteoporosis type II, and both are related in terms of fat gain at the expense of bone mass, irrespective of gender (Feng & McDonald, 2011; Horstman et al., 2012). In our study, despite the use of young animals that could be considered as a limitation, it was confirmed that the development of osteoporosis induced by orchietomy resulted in reduced osteoblast differentiation concomitantly with the increased adipogenic potential of MSCs. Besides, we demonstrated the same pattern in terms of osteoblast differentiation and adipogenic potential in osteoblasts cultured in a conditioned medium of osteoblasts previously cocultured with adipocytes. These findings suggested that adipocytes differentiated from adipose tissue MSCs could induce modifications

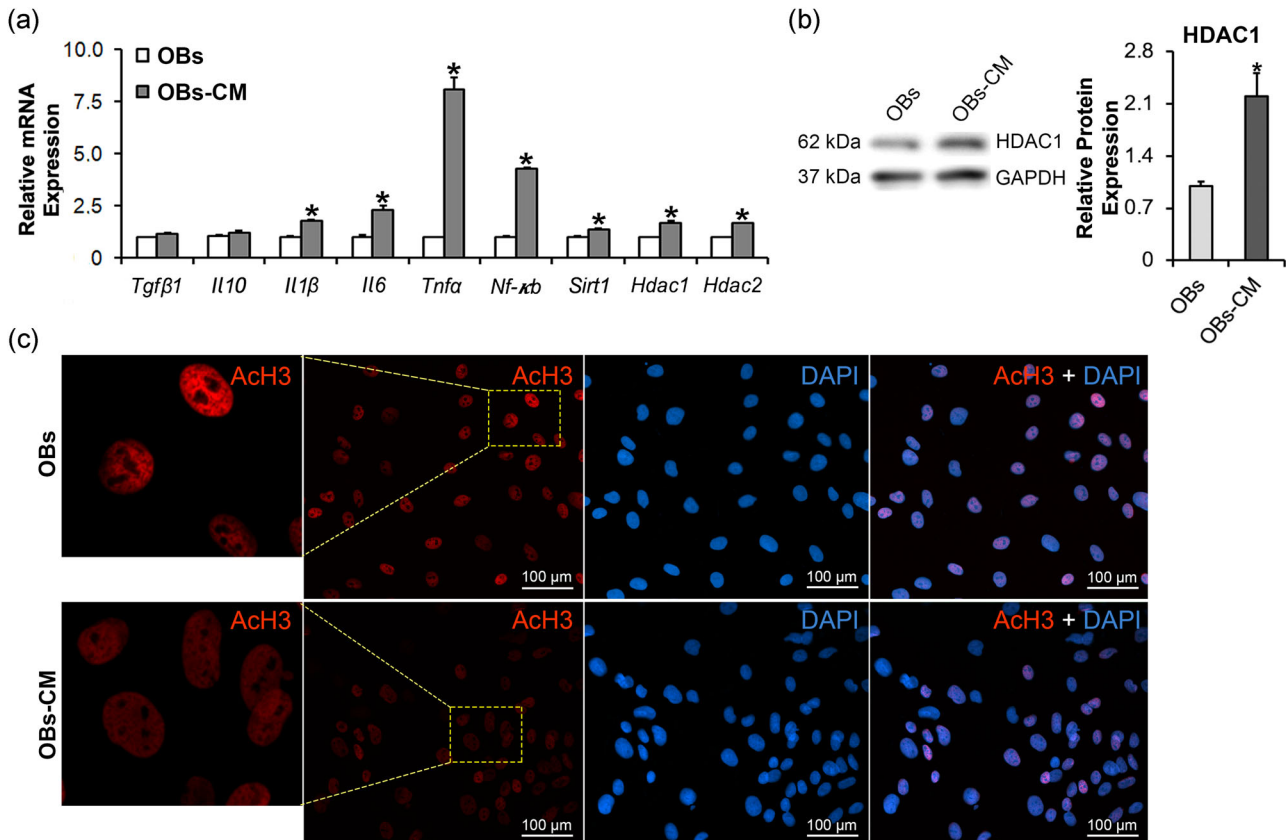


FIGURE 4 Effect of adipocytes (conditioned medium) on the expression of cytokines, histone deacetylases, and ACh3 by osteoblasts differentiated from MSCs. mRNA expression of the cytokines *Tgfb1*, *Il10*, *Il1β*, *Il-6*, *NF-κB*, *TNF-α*, and *Sirt1*, and histone deacetylases *Hdac1* and *Hdac2* on Day 10 (a), HDAC1 protein expression on Day 12 (b), and ACh3 protein expression on Day 12 (c) of osteoblasts cultured in nonconditioned medium (OBs) and osteoblasts cultured in conditioned medium (OBs-CM). The data of mRNA ($n = 3$) are presented as mean \pm standard deviation. ACh3, acetyl-histone 3; GAPDH, glyceraldehyde 3-phosphate dehydrogenase; HDAC, histone deacetylase; MSC, mesenchymal stromal cell; mRNA, messenger RNA. *Statistically significant differences between OBs and OBs-CM ($p \leq .05$)

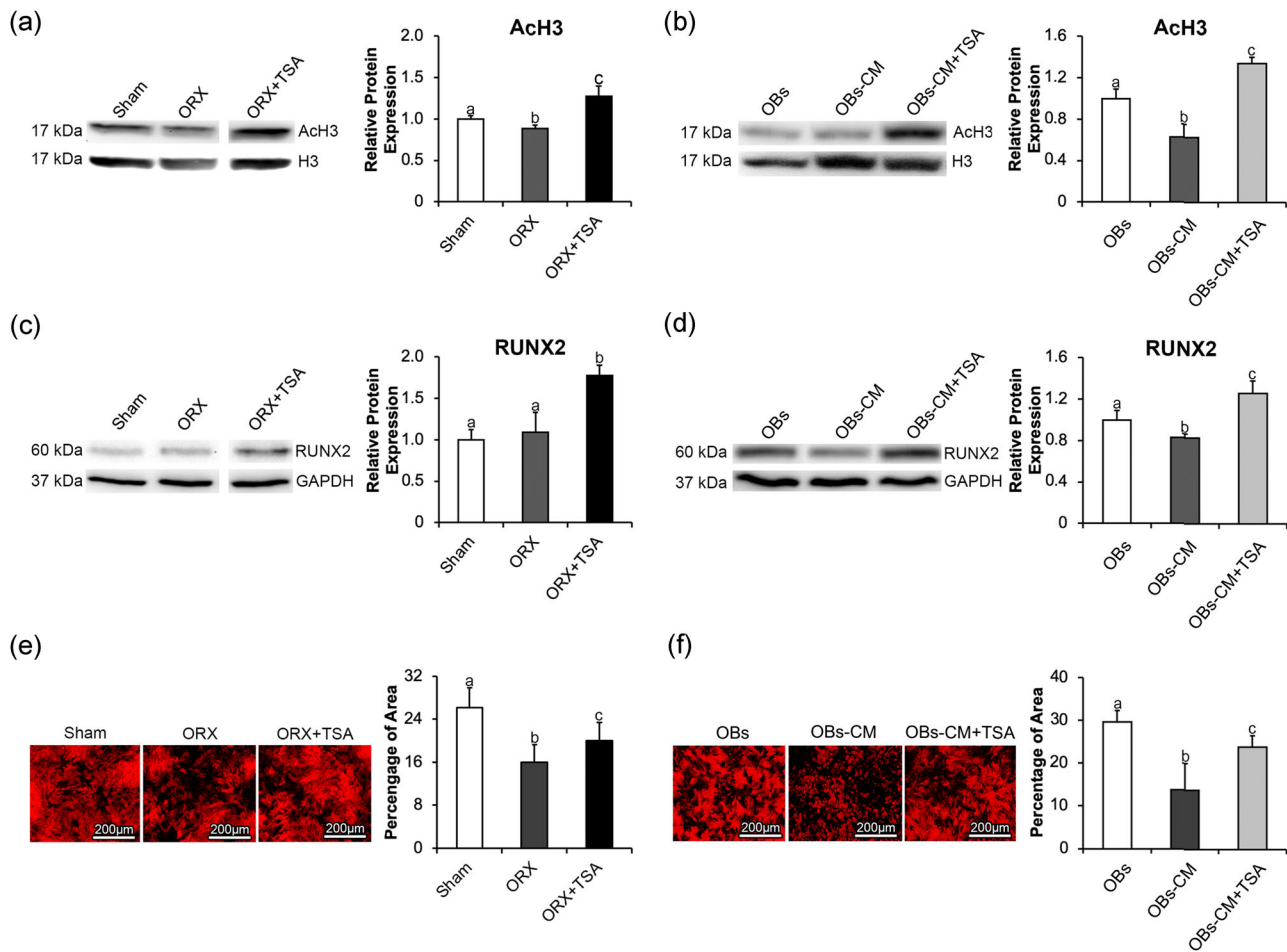


FIGURE 5 Role of acetyl-histone 3 (ACh3) in the osteoblast differentiation downregulation induced by orchietomy and adipocytes (conditioned medium). Effect of trichostatin A (TSA) on the protein expression of ACh3 (a,b) and RUNX2 (c,d) and in situ alkaline phosphatase (ALP) activity (e,f) of osteoblasts derived from Sham and orchietomy surgery (ORX) rats and on osteoblasts cultured in nonconditioned (OBs) and conditioned medium (OBs-CM) on Day 11. The data on protein expression ($n = 3$) and in situ ALP activity (average of five random stained areas of three wells, $n = 3$) are presented as mean \pm standard deviation. The space between the last and middle band (a,c) indicates splicing for the purpose of the presentation. *Statistically significant differences among osteoblasts derived from either Sham, ORX, and ORX treated with TSA or among OBs, OBs-CM, and OBs-CM treated with TSA ($p \leq .05$)

in the intracellular machinery of osteoblasts and that the negative impact of osteoporosis on bone mass is due to not only an imbalance of MSCs fate but also to an impairment of osteoblast differentiation induced by adipocytes (Abuna et al., 2016; L. Hu et al., 2018). Considering that the adipose tissue from bone marrow contains a heterogeneous cell population that may be affected by several pathophysiological conditions with consequences to the function of adipocytes (Aparisi Gómez et al., 2020), the extrapolation of our results to all these situations is complex, as, in our study, the adipocytes had differentiated from the adipose tissue MSCs of healthy animals. Additionally, it remains to be determined whether the osteoblast modifications induced by adipocytes significantly contribute to the bone loss in osteoporosis, if these modifications are permanent, and by what means can these modifications be reverted. The latter would open new therapeutic possibilities to treat osteoporosis.

As the participation of cytokines in bone loss induced by osteoporosis is well documented, and we too confirmed that some of them,

such as *TNF- α* and *NF- κ B* (Figure S3), are upregulated in osteoblasts under osteoporotic condition, we focused our study on epigenetic mechanisms that could be involved in the inhibition of osteoblast differentiation induced by osteoporosis. It has been shown that bone loss cannot be induced by gene polymorphisms alone but is also influenced by the epigenetic regulation of gene and protein expression without changes in the inherited DNA sequence (Hamam et al., 2014; Hsu & Kiel, 2012; Huang et al., 2010). This machinery includes DNA methylation, post-transcriptional microRNA regulation, and posttranslational histone modifications (Gibney & Nolan, 2010). Histone acetylation, mediated by histone acetyltransferases, is a widely studied histone modification responsible for transcriptional activation, whereas HDACs are transcriptional repressors promoting the loss of acetylation (Zardo et al., 2008). As the class II HDACs, *Hdac1* and *Hdac2* mRNAs, and HDAC1 protein were upregulated in both osteoblasts from osteoporotic animals and osteoblasts cultured in the conditioned medium, we analyzed and confirmed the lower expression of the ACh3 at Lys9 residue (H3K9ac), revealing a

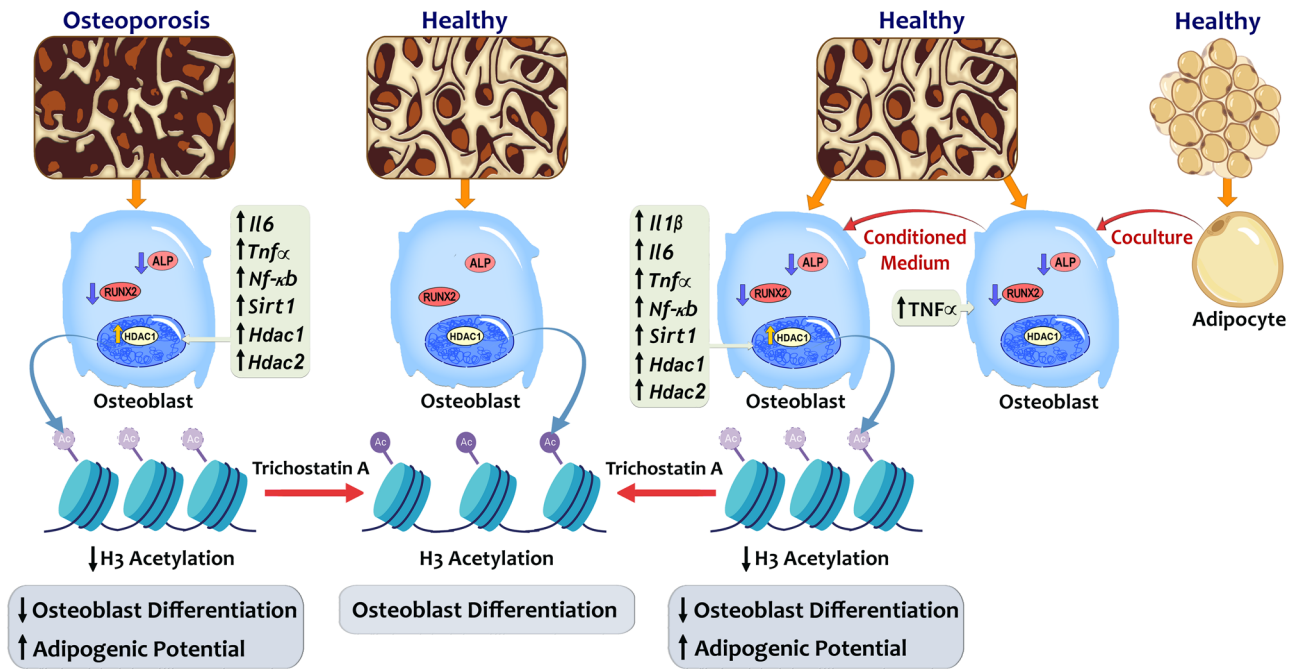


FIGURE 6 Schematic representation of the main findings of this study. It is demonstrated that osteoblasts retain the memory of the negative effect of their interaction with adipocytes that inhibits the differentiation of other osteoblasts, at least partly, through the same cellular mechanism as osteoporosis, that is, by reducing acetyl-histone 3

plausible epigenetic mechanism to explain the reduced osteoblast differentiation induced by osteoporosis as well as by the in vitro model of the conditioned medium. Interestingly, the reduced ACh3 expression induced by osteoporosis was observed even after taking cells out of the in vivo osteoporotic condition and exposing them to an in vitro cell culture environment, probably due to the epigenetic adaptation of the cells induced by osteoporosis.

Acetylation of specific lysine residues is associated with the promotion of transcription, DNA replication through the synthesis of new histones and mature chromatin assembly (Kimura & Horikoshi, 1998). Specifically, H3K9ac acts on chromatin assembly by recruiting transcriptional modulators with bromodomains or tandem PHD domains (Sobel et al., 1995; Zhao et al., 2007). Although the specific role of acetylation on bone diseases remains unclear, the consequence of aberrant lysine acetylation may be highlighted through deacetylation studies. It has been demonstrated that the deletion of HDAC1 in zebrafish produces severe defects in skeletogenesis due to dysregulation of the Wnt signaling pathway, and that Runx2 is regulated by HDAC4 to promote skeletal development (Pillai et al., 2004; Vega et al., 2004). Additionally, *Hdac1* and *Hdac2* transcripts are downregulated in normal osteoblastogenesis (Lee et al., 2006), and therefore, the higher expression of *Hdac1* and *Hdac2* could be involved in the downregulation of ACh3 triggered by osteoporosis and the conditioned medium that resulted in the impaired osteoblast differentiation reported in our study. To investigate this, osteoblasts were treated with TSA, an HDAC inhibitor that binds to the zinc-containing catalytic site of HDAC. Confirming our hypothesis, TSA treatment restored the expression of ACh3 and the downregulated osteoblast differentiation caused by osteoporosis and the

conditioned medium, proving that our in vitro model mimicked the cellular mechanisms by which osteoporosis impairs osteoblast differentiation. Corroborating the positive effect of TSA on osteoblasts, it was demonstrated that the histone hyperacetylation at the osteocalcin gene promoter, observed during osteoblast differentiation, can be increased by HDAC inhibition (X. Hu et al., 2013; Shen et al., 2003; Xu et al., 2013). Additionally, TSA may upregulate Runx2 expression and ALP activity and accelerate calcium deposition in cultures of osteoblastic cells (Schroeder & Westendorf, 2005).

We have reported the inhibitory effect of osteoporosis on osteoblast differentiation. Also, by creating an in vitro model using the conditioned medium of osteoblasts cocultured with adipocytes, it was demonstrated that osteoblasts retained their memory of the negative impact of their interaction with adipocytes. To the best of our knowledge, it was an unknown harmful effect of osteoporosis. Additionally, our results revealed the involvement of ACh3 in bone homeostasis, as its reduction, induced by osteoporosis and indirectly by adipocytes (conditioned medium), impaired osteoblast differentiation that was recovered by an HDAC inhibitor. Together, these findings indicated that ACh3 might be a target for future studies focused on epigenetic-based therapies to treat bone diseases.

ACKNOWLEDGMENTS

The authors thank Adriana L. G. Almeida, Fabiola S. Oliveira, and Milla S. Tavares for technical assistance during the research. This study was supported by the State of São Paulo Research Foundation (FAPESP, Brazil, #2016/14171-0, 2016/14711-4, 2017/12622-7, and 2018/13290-0), National Council for Scientific and Technological

Development (CNPq, Brazil, #303464/2016-0), and Coordination of Improvement of Higher Education Personnel (CAPES, Brazil). The English language review was carried out by ENAGO (www.enago.com) funded by FAPESP (#2018/17356-6).

DATA AVAILABILITY STATEMENT

The research data that supports the results of this study are available upon request from the corresponding author.

ORCID

Adalberto L. Rosa  <http://orcid.org/0000-0002-6495-2778>

Marcio M. Beloti  <http://orcid.org/0000-0003-0149-7189>

REFERENCES

- Abuna, R. P., de Oliveira, F. S., de S Santos, T., Guerra, T. R., Rosa, A. L., & Beloti, M. M. (2016). Participation of TNF- α in inhibitory effects of adipocytes on osteoblast differentiation. *Journal of Cellular Physiology*, 231, 204–214. <https://doi.org/10.1002/jcp.25073>
- Al Saedi, A., Chen, L., Phu, S., Vogrin, S., Miao, D., Ferland, G., Gaudreau, P., & Duque, G. (2020). Age-related increases in marrow fat volumes have regional impacts on bone cell numbers and structure. *Calcified Tissue International*, 107, 126–134. <https://doi.org/10.1007/s00223-020-00700-8>
- Aparisi Gómez, M. P., Ayuso Benavent, C., Simoni, P., Aparisi, F., Guglielmi, G., & Bazzocchi, A. (2020). Fat and bone: The multiperspective analysis of a close relationship. *Quantitative Imaging in Medicine and Surgery*, 10, 1614–1635. <https://doi.org/10.21037/qims.2020.01.11>
- Bennett, J. H., Joyner, C. J., Triffitt, J. T., & Owen, M. E. (1991). Adipocytic cells cultured from marrow have osteogenic potential. *Journal of Cell Science*, 99, 131–139.
- Bouxsein, M. L., Boyd, S. K., Christiansen, B. A., Guldborg, R. E., Jepsen, K. J., & Müller, R. (2010). Guidelines for assessment of bone microstructure in rodents using micro-computed tomography. *Journal of Bone and Mineral Research*, 25, 1468–1486. <https://doi.org/10.1002/jbmr.141>
- Dempster, D. W., Compston, J. E., Drezner, M. K., Glorieux, F. H., Kanis, J. A., Malluche, H., Meunier, P. J., Ott, S. M., Recker, R. R., & Parfitt, A. M. (2013). Standardized nomenclature, symbols, and units for bone histomorphometry: A 2012 update of the report of the ASBMR Histomorphometry Nomenclature Committee. *Journal of Bone and Mineral Research*, 28, 2–17. <https://doi.org/10.1002/jbmr.1805>
- Fani, N., Ziadlou, R., Shahhoseini, M., & Baghaban Eslaminejad, M. (2016). Comparative epigenetic influence of autologous versus fetal bovine serum on mesenchymal stem cells through in vitro osteogenic and adipogenic differentiation. *Experimental Cell Research*, 344, 176–182. <https://doi.org/10.1016/j.yexcr.2015.10.009>
- Feigenson, M., Shull, L. C., Taylor, E. L., Camilleri, E. T., Riester, S. M., van Wijnen, A. J., Bradley, E. W., & Westendorf, J. J. (2017). Histone deacetylase 3 deletion in mesenchymal progenitor cells hinders long bone development. *Journal of Bone and Mineral Research*, 32, 2453–2465. <https://doi.org/10.1002/jbmr.3236>
- Feng, X., & McDonald, J. M. (2011). Disorders of bone remodeling. *Annual Review of Pathology*, 6, 121–145. <https://doi.org/10.1146/annurev-pathol-011110-130203>
- Freitas, G., Souza, A., Lopes, H., Trevisan, R., Oliveira, F., Fernandes, R., Ferreira, F., Ros, F., Beloti, M., & Rosa, A. (2020). Mesenchymal stromal cells derived from bone marrow and adipose tissue: Isolation, culture, characterization and differentiation. *Bio-protocol*, 10, e3534. <https://doi.org/10.21769/BioProtoc.3534>
- Gibney, E. R., & Nolan, C. M. (2010). Epigenetics and gene expression. *Heredity*, 105, 4–13. <https://doi.org/10.1038/hdy.2010.54>
- Gregory, C. A., Gunn, W. G., Peister, A., & Prockop, D. J. (2004). An alizarin red-based assay of mineralization by adherent cells in culture: Comparison with cetylpyridinium chloride extraction. *Analytical Biochemistry*, 329, 77–84. <https://doi.org/10.1016/j.ab.2004.02.002>
- Hahn, B. H. (1988). Osteoporosis: Diagnosis and management. *Bulletin on the Rheumatic Diseases*, 38, 1–9.
- Hamam, D., Ali, D., Vishnubalaji, R., Hamam, R., Al-Nbaheen, M., Chen, L., Kassem, M., Aldahmash, A., & Alajez, N. M. (2014). microRNA-320/RUNX2 axis regulates adipocytic differentiation of human mesenchymal (skeletal) stem cells. *Cell Death and Disease*, 5, e1499. <https://doi.org/10.1038/cddis.2014.462>
- Han, Y., You, X., Xing, W., Zhang, Z., & Zou, W. (2018). Paracrine and endocrine actions of bone-the functions of secretory proteins from osteoblasts, osteocytes, and osteoclasts. *Bone Research*, 6, 16. <https://doi.org/10.1038/s41413-018-0019-6>
- Horstman, A. M., Dillon, E. L., Urban, R. J., & Sheffield-Moore, M. (2012). The role of androgens and estrogens on healthy aging and longevity. *The Journals of Gerontology. Series A, Biological Sciences and Medical Sciences*, 67, 1140–1152. <https://doi.org/10.1093/gerona/gls068>
- Hsu, Y. H., & Kiel, D. P. (2012). Clinical review: Genome-wide association studies of skeletal phenotypes: What we have learned and where we are headed. *The Journal of Clinical Endocrinology and Metabolism*, 97, E1958–E1977. <https://doi.org/10.1210/jc.2012-1890>
- Hu, L., Yin, C., Zhao, F., Ali, A., Ma, J., & Qian, A. (2018). Mesenchymal stem cells: Cell fate decision to osteoblast or adipocyte and application in osteoporosis treatment. *International Journal of Molecular Sciences*, 19, 360. <https://doi.org/10.3390/ijms19020360>
- Hu, X., Zhang, X., Dai, L., Zhu, J., Jia, Z., Wang, W., Zhou, C., & Ao, Y. (2013). Histone deacetylase inhibitor trichostatin A promotes the osteogenic differentiation of rat adipose-derived stem cells by altering the epigenetic modifications on Runx2 promoter in a BMP signaling-dependent manner. *Stem Cells and Development*, 22, 248–255. <https://doi.org/10.1089/scd.2012.0105>
- Huang, J., Zhao, L., Xing, L., & Chen, D. (2010). MicroRNA-204 regulates Runx2 protein expression and mesenchymal progenitor cell differentiation. *Stem Cells*, 28, 357–364. <https://doi.org/10.1002/stem.288>
- Huynh, N. C., Everts, V., & Ampornaramveth, R. S. (2017). Histone deacetylases and their roles in mineralized tissue regeneration. *Bone Reports*, 7, 33–40. <https://doi.org/10.1016/j.bonr.2017.08.001>
- Huynh, N. C., Everts, V., Nifuji, A., Pavasant, P., & Ampornaramveth, R. S. (2017). Histone deacetylase inhibition enhances in-vivo bone regeneration induced by human periodontal ligament cells. *Bone*, 95, 76–84. <https://doi.org/10.1016/j.bone.2016.11.017>
- Justesen, J., Stenderup, K., Ebbesen, E. N., Mosekilde, L., Steiniche, T., & Kassem, M. (2001). Adipocyte tissue volume in bone marrow is increased with aging and in patients with osteoporosis. *Biogerontology*, 2, 165–171. <https://doi.org/10.1023/a:1011513223894>
- Kimura, A., & Horikoshi, M. (1998). How do histone acetyltransferases select lysine residues in core histones? *FEBS Letters*, 431, 131–133. [https://doi.org/10.1016/s0014-5793\(98\)00752-2](https://doi.org/10.1016/s0014-5793(98)00752-2)
- Kotrych, D., Dziedziczko, V., Safranow, K., Sroczynski, T., Staniszewska, M., Juzyszyn, Z., & Pawlik, A. (2016). TNF- α and IL10 gene polymorphisms in women with postmenopausal osteoporosis. *European Journal of Obstetrics, Gynecology, and Reproductive Biology*, 199, 92–95. <https://doi.org/10.1016/j.ejogrb.2016.01.037>
- Lee, H. W., Suh, J. H., Kim, A. Y., Lee, Y. S., Park, S. Y., & Kim, J. B. (2006). Histone deacetylase 1-mediated histone modification regulates osteoblast differentiation. *Molecular Endocrinology*, 20, 2432–2443. <https://doi.org/10.1210/me.2006-0061>
- Manolagas, S. C., Bellido, T., & Jilka, R. L. (1995). New insights into the cellular, biochemical, and molecular basis of postmenopausal and senile osteoporosis: Roles of IL-6 and gp130. *International Journal of Immunopharmacology*, 17, 109–116. [https://doi.org/10.1016/0192-0561\(94\)00089-7](https://doi.org/10.1016/0192-0561(94)00089-7)
- Meunier, P., Aaron, J., Edouard, C., & Vignon, G. (1971). Osteoporosis and the replacement of cell populations of the marrow by adipose tissue. A quantitative study of 84 iliac bone biopsies. *Clinical Orthopaedics and*

- Related Research*, 80, 147–154. <https://doi.org/10.1097/00003086-197110000-00021>
- Montecino, M., Stein, G., Stein, J., Zaidi, K., & Aguilar, R. (2015). Multiple levels of epigenetic control for bone biology and pathology. *Bone*, 81, 733–738. <https://doi.org/10.1016/j.bone.2015.03.013>
- Muruganandan, S., Roman, A. A., & Sinal, C. J. (2009). Adipocyte differentiation of bone marrow-derived mesenchymal stem cells: Cross talk with the osteoblastogenic program. *Cellular and Molecular Life Sciences*, 66, 236–253. <https://doi.org/10.1007/s00018-008-8429-z>
- Noda, M., Yoon, K., Rodan, G. A., & Koppel, D. E. (1987). High lateral mobility of endogenous and transfected alkaline phosphatase: A phosphatidylinositol-anchored membrane protein. *The Journal of Cell Biology*, 105, 1671–1677. <https://doi.org/10.1083/jcb.105.4.1671>
- Pillai, R., Coverdale, L. E., Dubey, G., & Martin, C. C. (2004). Histone deacetylase 1 (HDAC-1) required for the normal formation of craniofacial cartilage and pectoral fins of the zebrafish. *Developmental Dynamics*, 231, 647–654. <https://doi.org/10.1002/dvdy.20168>
- Riggs, B. L., Melton, L. J., Robb, R. A., Camp, J. J., Atkinson, E. J., McDaniel, L., Amin, S., Rouleau, P. A., & Khosla, S. (2008). A population-based assessment of rates of bone loss at multiple skeletal sites: Evidence for substantial trabecular bone loss in young adult women and men. *Journal of Bone and Mineral Research*, 23, 205–214. <https://doi.org/10.1359/jbmr.071020>
- Rosen, C. J., Ackert-Bicknell, C., Rodriguez, J. P., & Pino, A. M. (2009). Marrow fat and the bone microenvironment: Developmental, functional, and pathological implications. *Critical Reviews in Eukaryotic Gene Expression*, 19, 109–124. <https://doi.org/10.1615/critrevukargeneexpr.v19.i2.20>
- Rosen, C. J., & Bouxsein, M. L. (2006). Mechanisms of disease: Is osteoporosis the obesity of bone? *Nature Clinical Practice. Rheumatology*, 2, 35–43. <https://doi.org/10.1038/ncprheum0070>
- Schroeder, T. M., & Westendorf, J. J. (2005). Histone deacetylase inhibitors promote osteoblast maturation. *Journal of Bone and Mineral Research*, 20, 2254–2263. <https://doi.org/10.1359/JBMR.050813>
- Shen, J., Hovhannisyann, H., Lian, J. B., Montecino, M. A., Stein, G. S., Stein, J. L., & Van Wijnen, A. J. (2003). Transcriptional induction of the osteocalcin gene during osteoblast differentiation involves acetylation of histones h3 and h4. *Molecular Endocrinology*, 17, 743–756. <https://doi.org/10.1210/me.2002-0122>
- Sobel, R. E., Cook, R. G., Perry, C. A., Annunziato, A. T., & Allis, C. D. (1995). Conservation of deposition-related acetylation sites in newly synthesized histones H3 and H4. *Proceedings of the National Academy of Sciences of the United States of America*, 92, 1237–1241. <https://doi.org/10.1073/pnas.92.4.1237>
- Takada, I., Suzawa, M., Matsumoto, K., & Kato, S. (2007). Suppression of PPAR transactivation switches cell fate of bone marrow stem cells from adipocytes into osteoblasts. *Annals of the New York Academy of Sciences*, 1116, 182–195. <https://doi.org/10.1196/annals.1402.034>
- Tyagi, A. M., Srivastava, K., Mansoori, M. N., Trivedi, R., Chattopadhyay, N., & Singh, D. (2012). Estrogen deficiency induces the differentiation of IL-17 secreting Th17 cells: A new candidate in the pathogenesis of osteoporosis. *PLOS One*, 7, e44552. <https://doi.org/10.1371/journal.pone.0044552>
- Vega, R. B., Matsuda, K., Oh, J., Barbosa, A. C., Yang, X., Meadows, E., McAnally, J., Pomajzl, C., Shelton, J. M., Richardson, J. A., Karsenty, G., & Olson, E. N. (2004). Histone deacetylase 4 controls chondrocyte hypertrophy during skeletogenesis. *Cell*, 119, 555–566. <https://doi.org/10.1016/j.cell.2004.10.024>
- Vondracek, S. F., & Linnebur, S. A. (2009). Diagnosis and management of osteoporosis in the older senior. *Clinical Interventions in Aging*, 4, 121–136. <https://doi.org/10.2147/cia.s4965>
- Xu, S., de Veirman, K., Evans, H., Santini, G. C., Vande Broek, I., Leleu, X., de Becker, A., van Camp, B., Croucher, P., Vanderkerken, K., & van Riet, I. (2013). Effect of the HDAC inhibitor vorinostat on the osteogenic differentiation of mesenchymal stem cells in vitro and bone formation in vivo. *Acta Pharmacologica Sinica*, 34, 699–709. <https://doi.org/10.1038/aps.2012.182>
- Zardo, G., Cimino, G., & Nervi, C. (2008). Epigenetic plasticity of chromatin in embryonic and hematopoietic stem/progenitor cells: Therapeutic potential of cell reprogramming. *Leukemia*, 22, 1503–1518. <https://doi.org/10.1038/leu.2008.141>
- Zarrow, M. X., Yochim, J. M., McCarthy, J. L., & Sanborn, R. C. (1964). *Experimental Endocrinology: A sourcebook of basic techniques* (pp. 136–137). Academic Press.
- Zhao, X. D., Han, X., Chew, J. L., Liu, J., Chiu, K. P., Choo, A., Orlov, Y. L., Sung, W. K., Shahab, A., Kuznetsov, V. A., Bourque, G., Oh, S., Ruan, Y., Ng, H. H., & Wei, C. L. (2007). Whole-genome mapping of histone H3 Lys4 and 27 trimethylations reveals distinct genomic compartments in human embryonic stem cells. *Cell Stem Cell*, 1, 286–298. <https://doi.org/10.1016/j.stem.2007.08.004>
- Zippo, A., Serafini, R., Rocchigiani, M., Pennacchini, S., Krepelova, A., & Oliviero, S. (2009). Histone crosstalk between H3S10ph and H4K16ac generates a histone code that mediates transcription elongation. *Cell*, 138, 1122–1136. <https://doi.org/10.1016/j.cell.2009.07.031>

SUPPORTING INFORMATION

Additional supporting information may be found online in the Supporting Information section.

How to cite this article: Abuna RPF, Almeida LO, Souza ATP, et al. Osteoporosis and osteoblasts cocultured with adipocytes inhibit osteoblast differentiation by downregulating histone acetylation. *J Cell Physiol*. 2020;1–12. <https://doi.org/10.1002/jcp.30131>